

# Matter

Article



We show in this paper that the magnitude of Rashba coefficients in different compounds is not well correlated with the magnitude of the SOC, and that the hallmark of strong Rashba coefficient is the appearance of energy band anti-crossing of the Rashba split bands. This has a few immediate consequences: First, because all topological insulators must have band anti-crossing, we show that all non-centrosymmetric topological insulators having non-zero electric dipole (i.e., topological insulators [TIs] that can have a Rashba effect) must be strong Rashba compounds. This provides a causal physical explanation for previous occasional observations of TIs having large Rashba coefficients and establishes a new cross-functionality: topological Rashba insulators (TRIs). Searching current databases of TI compounds for TI members that are also non-centrosymmetric with non-zero electric dipole predicts a few TRIs such as  $\text{Sb}_2\text{Te}_2\text{Se}$  and  $\text{TlN}$  with calculated large  $a_R$  of 3.88 eVÅ and 2.64 eVÅ in the valence bands, respectively. Second, we show that the anti-crossing theory of the Rashba scale can be used to identify new strong Rashba compounds by a different route—starting from known non-centrosymmetric structures—and identify those that also have anti-crossing bands. This approach led to identification of 34 previously synthesized strong Rashba compounds, including the already known  $\text{GeTe}$  and  $\text{BiTeI}$ , as well as compounds that have been previously synthesized but were unappreciated as Rashba compounds, let alone as strong Rashba compounds, such as  $\text{BiTeCl}$  ( $R\bar{3}m$ ),  $\text{PbS}$  ( $R3m$ ), and  $\text{K}_2\text{BaCdSb}_2$  ( $\text{Pmc}2_1$ ) with Rashba coefficients of 4.5, 4.6, and 5.3 eVÅ, respectively. Additionally, we also identify 165 weak Rashba compounds with Rashba parameter smaller than 1.2 eVÅ and Rashba spin splitting (RSS) larger than 1 meV (see

1). We hope that these predictions will be tested experimentally.

The theory above follows an inverse design approach: it predicts target properties based on physically motivated models that directly connect the existence of the

compounds that have larger than 1 meV spin splitting near the valence band maximum. This gives a broader impression of the distribution of the magnitude of the Rashba coefficients than what is currently available from isolated literature calculations. We focus on compounds with intrinsic dipoles ("bulk Rashba effect,"<sup>13</sup> denoted as R-1). We exclude (1) magnetic compounds (no time-reversal-symmetry) in which the Zeeman effect is observed instead, (2) surfaces or interfaces induced Rashba effects (the "R-0" effect),

a<sub>R</sub>

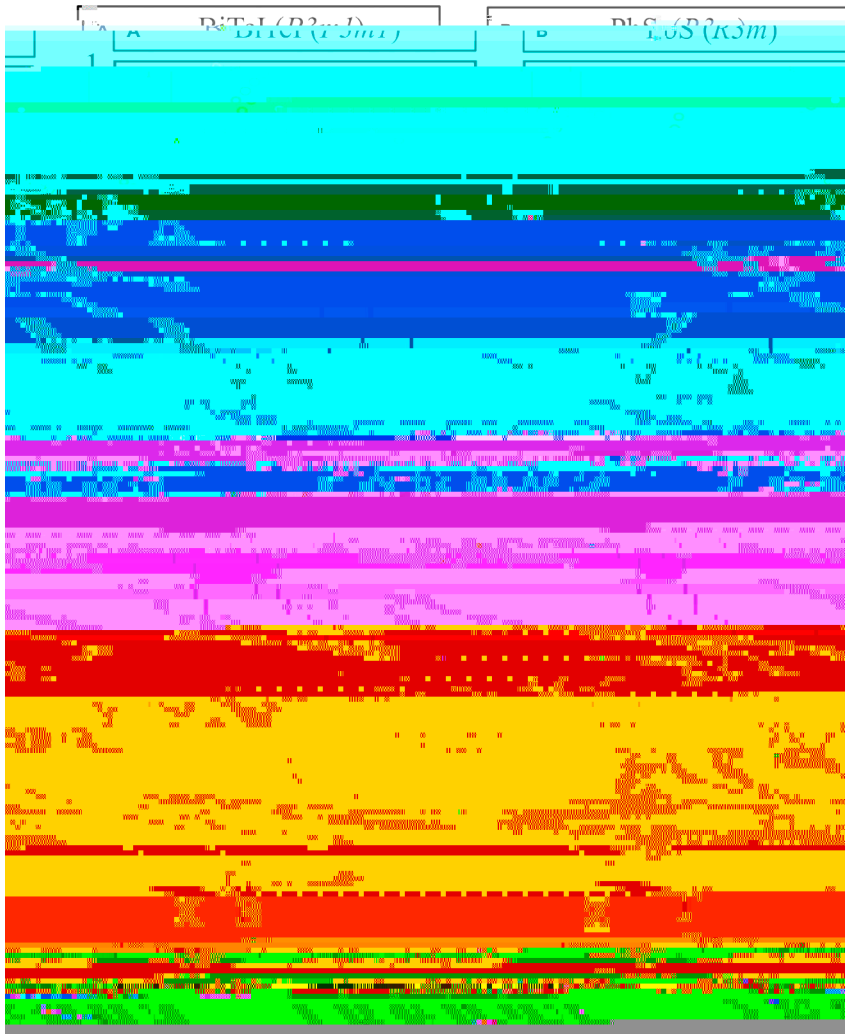
dispersed band, large momentum offset, and small RSS. These trends translate into large  $a_R$  (as in BiTeI) and small  $a_R$  (e.g.,  $\text{KSn}_2\text{Se}_4$ ).

In establishing whether these characteristic dispersion shapes also have a causal relationship with the magnitude of the Rashba coefficient in a given material (rather than in chemically dissimilar compounds such as  $\text{KSn}_2\text{Se}_4$  and BiTeI), it would be useful to control the dispersion shapes in the same material. Unfortunately this is not easy to do with DFT since the band shape can strongly depend on the atomic composition, lattice symmetry, and specific orbital interactions. Nevertheless, such shape engineering of band dispersion is readily possible within a tight-binding (TB) model which, however, does not have the additional virtue of material realism. Our strategy is therefore to use a simple TB model that enables transmuting the shape of Rashba band dispersion between the two prototypes of  $\text{KSn}_2\text{Se}_4$  and BiTeI, thus establishing what controls large versus small Rashba effects in a toy model, then use this TB identification of a metric in precise and material specific (3D) DFT calculations and observe how this reveals strong versus weak Rashba effects in real compounds. To this end, we constructed a model Hamiltonian including the minimal essential ingredients at play, namely: two orbitals at different sites, opposite effective mass sign, and SOC ( $t_{\text{SOC}}$ ). For illustrative purposes, we only consider s- and  $p_x$ -orbitals interacting through the hopping term  $t_{\text{sp}}$ .

proportional to the SOC (i.e.,  $a_R = 2at_{\text{soc}}$ ), and decreases as the inter-orbital interaction increases, since orbitals are deformed by the atomic bonding.








(A) BiTeI, (B) PbS, (C) Sb<sub>2</sub>Se<sub>2</sub>Te, and (D) GeTe (codes 74501, 183243, 60963, and 56040 in the Inorganic Crystal Structure Database, respectively). The green and magenta color scales stand for the orbital contribution to the CBM and VBM at the time-reversal high-symmetry  $\Gamma$  k-points, respectively. These orbital contributions are shown for the conduction band minimum (CBM) and valence band maximum (VBM) at the time-reversal high-symmetry  $\Gamma$  k-points, respectively. These orbital contributions are shown for the conduction band minimum (CBM) and valence band maximum (VBM) at the time-reversal high-symmetry  $\Gamma$  k-points, respectively.

the unit cell to non-zero value. Thus, according to the proposed theory, all non-centrosymmetric TIs having local dipoles that add up to non-zero are strong Rashba compounds. This observation will be used below to explain previously puzzling observation of trends in Rashba effects in TIs and to identify compounds that have the cross-functional property of TIs while also being Rashba materials (TRIs).

Experimental evidence of trends in Rashba behavior in non-centrosymmetric TIs was observed in thin films of  $n$  formula units  $(\text{Bi}_2\text{Se}_3)_n$  of the TI  $\text{Bi}_2\text{Se}_3$  grown in a SiC substrate. Figure 1 shows the experimentally estimated Rashba coefficient for different repeat units  $n$  in  $(\text{Bi}_2\text{Se}_3)_n$  plotted against the estimated effective electric potentials that reflect the breaking of inversion symmetry (generated here by the

induced electric dipole of SiC substrate). As seen in , this electric potential changes when n increases, but it remains almost the same for n = 4 and n = 5, so both the SOC and the electric dipole are almost constant for these n values. This leaves unexplained the  $D_{aR} = 1.15 \text{ eVA}$

as TI candidates, Tang et al.

inter-atomic bonding, which can be distributed in such a way that the dipole

small in the reported lists, which is not related to existence of Rashba materials in nature. Indeed, we emphasize that these filters (band gap and NC space groups, lines c and d in ) are not conditions for the specific selection of either weak or strong Rashba compounds. The highlight here is that all selected TRIs are predicted to be strong Rashba compounds, as predicted by the proposed definition of the Rashba scale as a consequence of the existence of energy band anti-crossing.

The previous section looked for the interesting cross-functionality of TIs that are also Rashba compounds, starting from TIs and downselecting those that are Rashba like. The complementary search, ignored thus far, starts from Rashba compounds and downselects those that have anti-crossing bands even if they are not TIs. It turns out that the yield of this complementary search is much larger than that of the previous search.

As we will start from Rashba compounds, one needs to note that there are a few types of Rashba band splitting compounds: when the splitting is either between different valence bands, between different conduction bands, or between valence and conduction bands. For instance, as A shows for  $\text{KSr}_2\text{Se}_4$ , the interaction between the valence bands  $G_{1v}$  and  $G^0_{1v}$  along the G-X symmetry path is symmetry allowed, leading to a strong Rashba effect inside the valence bands. However, there is no anti-crossing between valence and conduction bands, so the Rashba effect at such a band edge is weak. Here, we are interested primarily in compounds featuring band edge Rashba splitting, i.e., near the VBM or CBM. To this end we will focus only on anti-crossing between these band edge states.

describes the selection strategy based on our design principles, which is divided into three filtering processes, shown in the vertical column in .

III provides more technical details on the selection strategies. We consider a database of Rashba R-1 compounds, i.e., in which the inversion symmetry is broken by dipoles generated by intrinsic polar atomic sites (steps 1 and 2 below). Such a database has not existed as yet and will be constructed below. After this we will downselect those Rashba compounds that have band anti-crossing (step 3 below). Our 3 steps are as follows.

- (1) Find non-magnetic gapped compounds calculated previously by DFT ( Iter 1 in ). Our starting point is the AFLOW-ICSD database (note that most compounds in ICSD have been previously synthesized), containing 20,831 unique compounds with less than 20 atoms per unit cell that were calculated by DFT (see for details). Next, we downselect ( Iter 1 in ) those compounds that have time-reversal symmetry (non-magnetic) resulting in 13,838 non-magnetic compounds, from which 6,355 are gapped non-magnetic compounds (band gap larger than 1 meV). We note that the aforementioned database used as magnetic configuration a ferromagnetic ordering.
- (2) Find the subset of non-magnetic gapped compounds that has non-centrosymmetric space group with at least one polar atomic site and non-zero dipole ( Iter 2 in

cancellation of dipole can be found in (III). This gives 867 compounds that are Rashba non-metals.

- (3) Sort out the subsets of Rashba non-metals with anti-crossing bands (type I Rashba) and with no anti-crossing bands (type II Rashba) (liter 3 in (III)). To do so we perform high-throughput DFT calculations including SOC of the band structure and spin texture for the 867 Rashba non-metals in order to identify anti-crossing bands and classify them into strong and weak Rashba compounds (DFT details are given in (III)). We find 286 Rashba compounds with spin splitting positioned within 30 meV or less

(see B). However, for anti-crossing bands, the orbital character for k-vectors smaller and larger than the momentum offset is expected to be different (see





identified compounds provide a platform for spin-conversion devices and the exploration of phenomena potentially hosted by Rashba compounds.

The DFT band structure calculations were performed using the Perdew-Burke-Ernzerhof generalized gradient approximation (PBE) exchange-correlation functional and the Hubbard on-site term  $U$  as implemented in the Vienna Ab-initio Simulation Package. We use the theoretical structures predicted in the AFLOW-database by initially setting the magnetic con

the k-point in which the sign of the derivatives changes (i.e., the momentum offset  $k_R$ ) and the value of the spin splitting ( $E_R$ ) to compute the Rashba coefficient, i.e.,  $a_R = 2E_R/k_R$

approximation leads to the same results expected in a  $k, p$  model (e.g., the Hamiltonian in (1)) using the L, S term (i.e., the Rashba term  $a_R s_y k_x$  in one-dimensional system), as we show below.

For  $k_y \neq 0$ , considering that  $t_{pp} = t_{pp}^{ll} = t_{pp}^{yy}$ , this Hamiltonian results in a very simplified expression for the  $p$ -orbital interaction, namely,

$$H_p \approx \epsilon_p + 2t_{pp} - t_{pp} a^2 k_x^2 - i 2t_{soc}^p k_x a$$

with opposite effective mass, as illustrated in the proposed 1D chain with two atomic species.

Note that we used here the  $s$ -orbitals as notation for states with total angular momentum equal to  $J = 1/2$ , and hence the discussion previously presented is for instance also extended to  $p_z$ -orbitals, which leads to a non-zero SOC. The pure  $s$ -orbitals should result in a zero RSS, since the SOC is zero. In fact, the obtained Hamiltonian  $H_{\text{eff}}$  is similar to that discussed in Acosta and Fazzio for the interaction between states with total angular momentum  $J = 1/2$  and  $J = 3/2$ .

Alex Zunger. Email address: .

This study did not generate new unique reagents.

All data needed to evaluate the conclusions in the paper are present in the paper and the . Additional data related to this paper may be requested from the authors.

Supplemental Information can be found online at .

The work at the University of Colorado at Boulder was supported by the National Science Foundation NSF Grant NSF-DMR-CMMT no. DMR-1724791. The work in Brazil was supported by the São Paulo Research Foundation FAPESP grant no. 17/02317-2 and by CNPq. C.M.A. and E.O. were supported by the São Paulo Research Foundation FAPESP grants 18/11856-7 and 18/1164

The authors declare no conflict of interest.

Received: January 13, 2020

Revised: March 25, 2020

Accepted: May 7, 2020

Published: July 1, 2020

1.

